

## ORIGINAL RESEARCH ARTICLE

A DFT+U Study of the Structural and Electronic Properties of Zinc-Doped Anatase TiO<sub>2</sub> NanomaterialShamsuddeen Sani Alhassan<sup>1</sup>  and Mahmud Abdulsalam<sup>1</sup> .<sup>1</sup>Department of Physics, Umaru Musa Yar'adua University, Katsina, Katsina State, Nigeria.

## ARTICLE HISTORY

Received December 06, 2023.

Accepted March 10, 2024.

Published March 30, 2024.

## ABSTRACT

This work reports a theoretical study on the structural and electronic properties of the anatase phase of titanium dioxide (TiO<sub>2</sub>) within the framework of density functional theory corrected for on-site coulomb interactions in strongly correlated materials (DFT+U). The exchange correlation was described by local density approximation (LDA). The optimized lattice parameters obtained for the pure anatase TiO<sub>2</sub> agree with the experimental data. Our results revealed that, after the zinc doping, the structure didn't change but there was a little expansion in the volume of the pure material. It was found that the doped structure's stability increases as the concentration of the dopant increases, but all the doped structures are stable. However, introducing the zinc dopant has significantly reduced the band gap of the pure anatase by 80.7 %, 80 %, and 78.6 % due to 0.25, 0.5, and 0.75 doping concentrations, respectively. This implies that the band gap energy increases as the doping concentration increases.

## KEYWORDS

Structural properties, Electronic properties, Titanium dioxide, Density functional theory, Doping.



© The authors. This is an Open Access article distributed under the terms of the Creative Commons Attribution 4.0 License (<http://creativecommons.org/licenses/by/4.0>)

## INTRODUCTION

Titanium dioxide (TiO<sub>2</sub>), also known as titania, is the only naturally occurring oxide of titanium at atmospheric pressure. It exists in three main polymorphs: rutile, anatase, and brookite. However, the brookite phase is very difficult to synthesize compared to the other two, so it is rarely studied (Beltran et al., 2006). Other high-pressure phases of TiO<sub>2</sub> have been reported (Kominami et al., 2000).

However, TiO<sub>2</sub> has been used for many years in various industrial and consumer goods, including paints, coatings, adhesives, paper and paperboard, plastics and rubbers, and printing inks. Subsequently, researchers have proven other potential applications of this material, such as in photocatalysis, dye-sensitized solar cells, sensors, hydrolysis, etc. (Fujishima et al., 1972; Tang et al., 1995; Bai et al., 2014; Al-Attafi et al., 2018; Qing et al., 2019; Sasanka et al., 2021). The excellent chemical stability, low cost, and non-toxicity of TiO<sub>2</sub> are some of the main factors that made it more attractive in the fields mentioned above.

Moreover, despite all the advantages of this material, some challenges still need to be addressed for more diverse applications. The wide band gap of TiO<sub>2</sub> (3.0 eV for rutile and 3.2 eV for anatase TiO<sub>2</sub>, respectively) (Daude et al., 1977; Takeshi et al., 2001) has limited its applicability in many fields. The photon absorption of semiconductors depends largely on their band gap energy. A material only

absorbs photons when the semiconducting band gap energy is lower than the photon energies. Due to its wide band gap, TiO<sub>2</sub> can only generate electron-hole pairs under ultra violet (UV) light. It is well known that solar light consists of only 5 % UV light; a large part of solar energy cannot be utilized (Dantong et al., 2015). Thus, this necessitates extending the light absorption of TiO<sub>2</sub> beyond the UV region.

Because of this, several works were reported theoretically and experimentally using both metal and non-metal dopants in engineering the material's band gaps, thereby extending the light absorption to at least the visible region. Some of the metal dopants used were Ag, Fe, V, Al, Pt, Cu, Cr, and Zn (Lee et al., 2005; Carneiro et al., 2005; Wu and Chen, 2004; Li and Li, 2001; Li and Li, 2002) and non-metals were N, S, C, B (Wu, et al., 2008; Takeshita et al., 2006; Yu et al., 2006; Treschev et al., 2008; Lettmann et al., 2001; Zaleska et al., 2007). However, a lot of density functional theory (DFT) based studies were reported explaining some important properties of TiO<sub>2</sub> which include but are not limited to Electronic band structure and optical properties of TiO<sub>2</sub> (Nura et al., 2019), phase stability in doped TiO<sub>2</sub> (Dorian et al., 2012). Nitrogen-doped TiO<sub>2</sub> was reported using DFT+U (GGA-PBE) formalism. The band gap was reduced by 0.6 eV (Navarra et al., 2022). A 0.89 eV reduction was reported using 5.6 % Cu doping on the (112) anatase TiO<sub>2</sub> surface through the GGA-PBE scheme (Sharma et al., 2023).

**Correspondence:** Shamsuddeen Sani Alhassan. Department of Physics, Umaru Musa Yar'adua University, Katsina, Katsina State, Nigeria. ✉ [shamsuddeen.sani@umyu.edu.ng](mailto:shamsuddeen.sani@umyu.edu.ng). Phone Number: +234 703 526 5877.

**How to cite:** Alhassan, S. S., & Abdulsalam, M. (2024). A DFT+U Study of the Structural and Electronic Properties of Zinc Doped Anatase TiO<sub>2</sub> Nanomaterial. *UMYU Scientifica*, 3(1), 186 – 191. <https://doi.org/10.56919/usci.2431.020>

In particular, zinc ion ( $\text{Zn}^{2+}$ ) has been reported to be one of the best dopants in  $\text{TiO}_2$  due to its low cost, provision of excess negative charge carriers, and low empty trap states (Meesombad et al., 2021). In addition to this, among all the transition metal ions,  $\text{Zn}^{2+}$  gives more effective doping with  $\text{TiO}_2$  because ionic radii of  $\text{Zn}^{2+}$  (0.74 Å) and  $\text{Ti}^{4+}$  ion (0.75 Å) are almost the same (Rauf et al., 2011). Therefore, the  $\text{Zn}^{2+}$  ion can readily replace the  $\text{Ti}^{4+}$  ion in the  $\text{TiO}_2$  lattice without altering the crystal structure (Aware and Jadhav, 2016). Recently, increasing interest has been in doping  $\text{TiO}_2$  nanostructured with  $\text{Zn}^{2+}$  ion. Zinc-doped  $\text{TiO}_2$  nanoparticles were reported using the solution combustion technique, narrower band gaps and slight particle refinement were observed in the nanoparticles with higher Zn concentration (Meesombad et al., 2021). However, a Zn-doped  $\text{TiO}_2$  film's higher photocatalytic activity compared with the undoped sample was reported using an acidic oxidation method and heat treatment process (Tuncay et al., 2022). Other DFT works reported a slight decrease in the band gap of the pure anatase  $\text{TiO}_2$  due to zinc doping (Othmen et al., 2021; Vivak et al., 2023).

However, despite all these, most of the theoretical works use the conventional DFT- which has been characterized by having a typical problem of underestimating the electronic band gaps of materials. One of the best methods of relieving this problem of the conventional DFT is by employing the DFT plus Hubbard correction U (DFT+U) method in strongly correlated systems.

Therefore, this work is centered on investigating the effect of zinc doping on the structural and electronic properties of anatase  $\text{TiO}_2$  within the framework of DFT+U formalism.

## MATERIAL AND METHOD

### Computational Method

The calculations were performed on the conventional cells of anatase  $\text{TiO}_2$  using first principle calculation based on

density functional theory plus Hubbard correction (DFT+U) as implemented in the QUANTUM ESPRESSO simulation package (Paola et al., 2009). We chose Hubbard value  $U = 7$  eV - which gave the band gap close to the experimental value. The local density approximation (LDA) parameterization of Perdew and Zunger (PZ) was employed in describing the exchange-correlation potential for both the undoped and doped structures. The plane wave basis sets with the maximum kinetic energy cut-off of 340 eV were used to expand the wave functions. The electron-ion core interaction was treated by ultrasoft pseudopotentials for Ti ( $3s^2 3p^6 4s^2 3d^2$ ), O ( $2s^2 2p^4$ ) and Zn ( $3s^2 3p^6 4s^2 3d^{10}$ ) valence orbitals as were all obtained in the pseudopotential files. The Brillouin zone integration was performed using the Monkhorst-Pack scheme (Monkhorst and Pack, 1976) with  $6 \times 6 \times 6$  k-points grids.

The cell dimensions and atomic positions were fully relaxed for all calculations using the Broyden-Fletcher-Goldfarb-Shannon (BFGS) algorithm until the forces acting on the atoms approached a zero value. The calculated electronic densities of states were found using denser k-point mesh.

The conventional cell used in the work has 12 atoms: 4 Ti atoms and 8 oxygen atoms. The substitutional doping was carried out at the Ti-atomic site. Thus, replacing one of the four Ti atoms with one Zn atom corresponds to 25% Zn doping ( $x=0.25$ ), replacing two Ti atoms with two Zn atoms corresponds to 50% Zn doping ( $x=0.5$ ), and three Ti atoms replaced by three Zn atoms corresponds to 75% Zn doping ( $x=0.75$ ).

## RESULTS AND DISCUSSION

### Structural Properties

The anatase phase of  $\text{TiO}_2$  exhibits a tetragonal crystal structure with space group  $I4_1/amd$ , as shown in Figure 1 below.

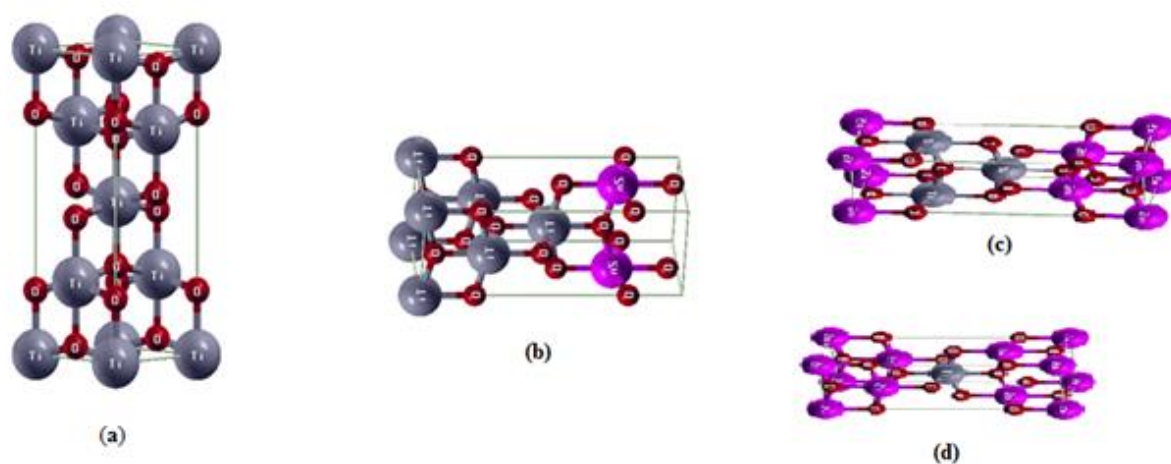


**Figure 1:** LDA + U Optimized Crystal Structures of (a) Pure Anatase  $\text{TiO}_2$  (b) 25 % Zn Doped  $\text{TiO}_2$  (c) 50 % Zn Doped  $\text{TiO}_2$  (d) 75 % Zn Doped  $\text{TiO}_2$

The optimized lattice parameters of the pure and doped models were calculated and shown in Table 1 below. It can be seen that the calculated lattice parameters of the pure anatase TiO<sub>2</sub> were in reasonable agreement with the experimentally reported data (Howard et al., 1991; Pascual et al., 1978). The percentage differences between the experimental data and our results were 1.79 % and 2.06 % for the lattice constants *a* and *c*, respectively. This has shown the reliability of the adopted method.

However, after the 25 % zinc doping, the lattice parameters were slightly decreased by 0.5 % and 0.1 % for *a* and *c* respectively. The little reduction of the lattice constants may be due to the imbalance of charges and slight variations of ionic radii of Zn<sup>2+</sup> and Ti<sup>4+</sup> ions. On the other hand, the unit cell volume was expanded by 0.74 %. This slight unit cell volume expansion after doping is similar to other theoretical reported work (Hao et al., 2017). Our calculation results revealed that, the other two doping models (50 % and 75 % zinc doping) have the same lattice parameters and unit cell volumes with 25 % zinc doping. This implies that a change in concentration of the dopant doesn't alter the lattice parameters or the unit cell volume.

To investigate the stability of the zinc-doped structures, we calculated the dopant formation energies of the zinc atom using equation (1) (Zhang et al., 2007). The dopant formation energy in this context is defined as the energy required to insert one zinc atom with a chemical potential

$\mu_{Zn}$  into the cell after removing one titanium atom with chemical potential  $\mu_{Ti}$  from the same position (Dorian et al., 2012).

$$E_f = E_{doped} - E_{undoped} + \mu_{Ti} - \mu_{Zn} \quad (1)$$

Where,  $E_{doped}$  is the DFT+U total energy of the zinc-doped TiO<sub>2</sub>,  $E_{undoped}$  is the DFT+U total energy of the pure TiO<sub>2</sub>,  $\mu_{Ti}$  is the chemical potential per atom of titanium bulk crystal and  $\mu_{Zn}$  is the chemical potential per atom of zinc bulk crystal. Following common practice (Zhang et al., 2007), the chemical potentials are calculated as the DFT total energy per atom in the bulk systems. The calculated dopant formation energies of the doped systems are shown in Table 1. All three doped structures are stable due to the possession of negative formation energies. However the 75 % zinc-doped structure has the lowest dopant formation energy and thus the most stable.

### Electronic Properties

The band gap values obtained for the pure and doped TiO<sub>2</sub> models (in this work) are compared with other DFT-reported studies, as shown in Table 2 below. It can be seen that the type of exchange-correlation approximation used greatly affects the band gap. However, the results obtained in the present work give the smallest band gap values for the doped systems compared to conventional DFT reported works.

**Table 1:** The LDA+U optimized lattice constants, dopant formation energies, and unit cell volumes of pure anatase TiO<sub>2</sub> and its zinc-doped models.

S/N	TiO <sub>2</sub> Models	Lattice Constants (Å)	Exp. lattice Constants(Å) (Howard et al.,1991; Pascual et al.,1978)	Dopant Formation Energy(E <sub>f</sub> ) (eV)	Unit Cell Volume (Å <sup>3</sup> )
1	Pure Anatase TiO <sub>2</sub>	a=b=3.717,c=9.3177	a=b= 3.7850, c= 9.5140	-	128.75
2	Ti <sub>1-x</sub> Zn <sub>x</sub> O <sub>2</sub> (x=0.25)	a=b=3.698,c=9.3068	-	-10.53	129.70
3	Ti <sub>1-x</sub> Zn <sub>x</sub> O <sub>2</sub> (x=0.50)	a=b=3.698,c=9.3068	-	-140.57	129.70
4	Ti <sub>1-x</sub> Zn <sub>x</sub> O <sub>2</sub> (x=0.75)	a=b=3.698,c=9.3068	-	-270.87	129.70

**Table 2:** Comparison between this work and other DFT works reported regarding the materials, type of exchange-correlation approximation (X-C) used, band gaps, and band gap reductions.

S/N	Material/Model	X-C Used	Band-gap (eV)	Band-gap Reduction (eV)	References
1	Pure TiO <sub>2</sub>	LDA + U	2.90	-	This work
2	25% Zn doped TiO <sub>2</sub>	LDA + U	0.56	2.34	This work
3	50% Zn doped TiO <sub>2</sub>	LDA + U	0.58	2.32	This work
4	75% Zn doped TiO <sub>2</sub>	LDA + U	0.62	2.28	This work
5	Pure TiO <sub>2</sub>	GGA	2.12	-	Vivek et al., 2023
6	6.5% Zn doped TiO <sub>2</sub>	GGA	1.73	0.39	Vivek et al., 2023
7	Pure TiO <sub>2</sub>	GGA + U	2.87	-	Vivek et al., 2023
8	6.5% Zn doped TiO <sub>2</sub>	GGA + U	2.60	0.27	Vivek et al., 2023
9	Pure TiO <sub>2</sub>	LDA	2.25	-	Othmen et al., 2021
10	2 % Zn doped TiO <sub>2</sub>	LDA	2.24	0.01	Othmen et al., 2021
11	4% Zn doped TiO <sub>2</sub>	LDA	1.94	0.31	Othmen et al., 2021
12	6% Zn doped TiO <sub>2</sub>	LDA	1.86	0.39	Othmen et al., 2021

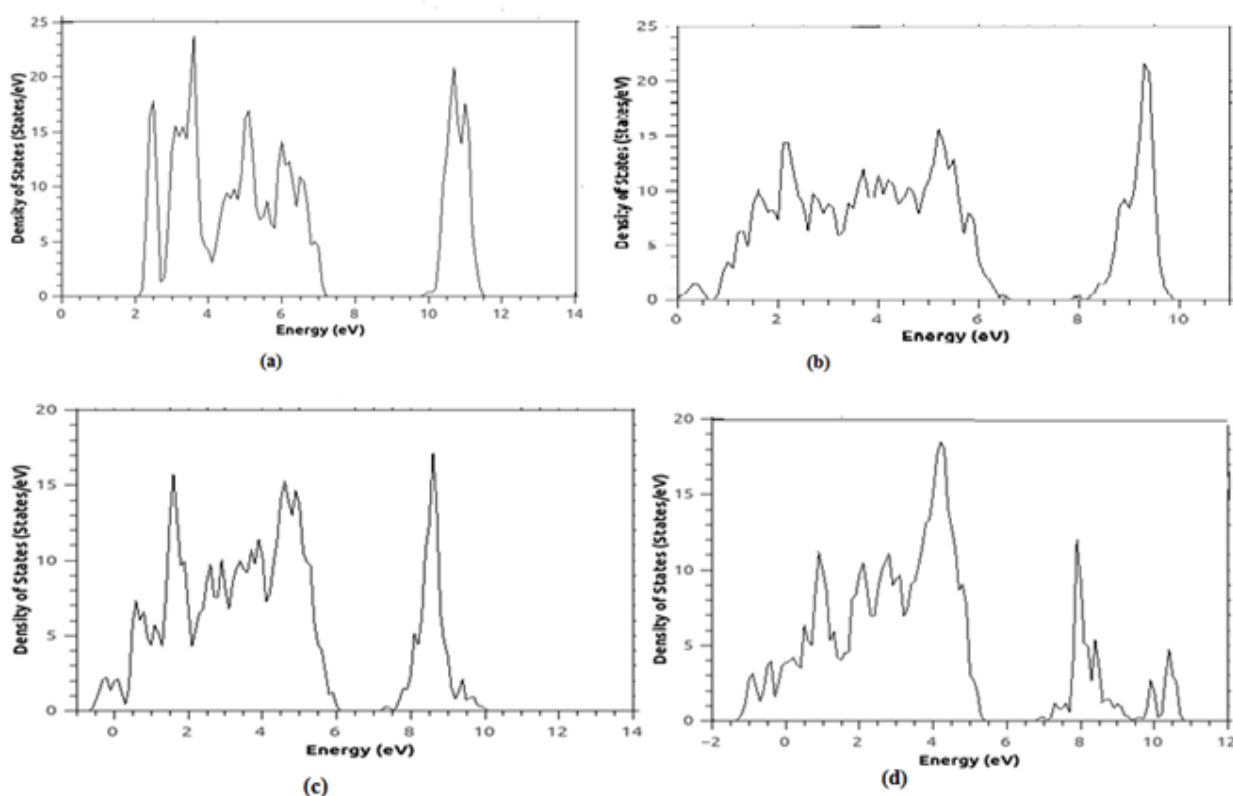
Figure 2(a) shows the DOS plot for the pure anatase TiO<sub>2</sub>. It can be seen that there are more states in the valence band than in the conduction band. The calculated DOS is zero between 7.04 eV and 9.95 eV, which is the forbidden gap. Thus, the calculated band gap energy of the pure anatase TiO<sub>2</sub> is 2.9 eV. This value is close to the experimental value of 3.2 eV (Daude et al., 1977; Takeshi et al., 2001) and exceeded the theoretical values of 1.94 eV and 2.07 eV (Landman et al., 2012; Nura et al., 2019).

Figure 2(b) displays the DOS of the 25 % zinc-doped TiO<sub>2</sub>. No states are available for occupation in the interval 5.54 eV to 6.10 eV; hence, the band gap is 0.56 eV. This is equivalent to an 80.7 % reduction compared to pure material. As shown from the plot, more states were introduced especially to the valence band.

However, the DOS plot of 50 % zinc-doped TiO<sub>2</sub> is shown in Figure 2(c). The zero states were observed between 4.88 eV and 5.45 eV. The calculated band gap of the material is 0.58 eV, which corresponds to an 80 % reduction compared to that of the pure anatase TiO<sub>2</sub>.

Figure 2(d) reveals the DOS of the 75 % zinc-doped material. Like other doped models, more states were contributed to the valence band. The calculated band gap is 0.62 eV, meaning that the pure anatase TiO<sub>2</sub> band gap was reduced by 78.6 %.

The 25 % zinc doping has the lowest band gap with the 75 % doping model having the highest. This implies that the band gap energy increases as the doping concentration increases.



**Figure 2:** Density of States (DOS) plots of the: (a) Pure anatase TiO<sub>2</sub> (b) 25 % Zn Doped TiO<sub>2</sub> (c) 50 % Zn Doped TiO<sub>2</sub> (d) 75 % Zn Doped TiO<sub>2</sub>

Therefore, it can be predicted that zinc doping significantly narrows the band gap of the pure anatase TiO<sub>2</sub> in agreement with the experimental findings and other DFT works (Meesombad et al., 2021; Othmen et al., 2021; Vivek et al., 2023).

## CONCLUSION

This paper reported the first principle study on the structural and electronic properties of anatase titanium dioxide (TiO<sub>2</sub>) based on density functional theory plus Hubbard corrections (DFT+U).

Firstly, about the structural properties, the optimized lattice parameters of the pure anatase TiO<sub>2</sub> agreed with the experimental values. There was no structural transition after the zinc doping, only that the pure material suffered a slight expansion in its volume. We found out that all the doped structures are stable with the 75 % zinc doped model being the most stable.

Secondly, zinc doping has significantly decreased the band gap of the pure anatase TiO<sub>2</sub> on the electronic properties. The 25 % zinc doping has the lowest band gap with the 75 % doping model having the highest. However, more states were also contributed after the doping especially in the valence band.

Conclusively, based on the results obtained, it can be predicted that the zinc-doped TiO<sub>2</sub> nanomaterial may be considered a very good candidate in photocatalysis and photovoltaic applications, among others.

## REFERENCES

- Al-Attafi, K., Nattestad, A., Wu, Q., Ide, Y., Yamauchi, Y., Dou, S. X., & Kim, J. H., (2018). The Effect of Amorphous TiO<sub>2</sub> in P25 on Dye-Sensitized Solar Cell Performance. *Chemical Communications*, 54,381-384. [[Crossref](#)]
- Aware, D.V. & Jadhav, S. S. (2016). Synthesis, Characterization and Photocatalytic Applications of Zn doped TiO<sub>2</sub> Nanoparticles by Sol-gel Method. *Applied Nanoscience*, 6, 965-972. [[Crossref](#)]
- Bai, J. & Zhou, B., (2014). Titanium Dioxide Nanomaterials for Sensor Applications. *Chemical Reviews*, 114, 10131-10176. [[Crossref](#)]
- Beltran, A., Gracia, L. & Andres, J. (2006). Density Functional Theory Study of the Brookite Surfaces and Phase Transitions Between Natural Titania Polymorphs. *Journal of physical chemistry B*, 110(46), 23417-23423. [[Crossref](#)]
- Carneiro J.O, Teixeira V., Portinha A., Dupak L., Magalhaes A. & Coutinho P. (2005). Study of the Deposition Parameters and Fe-dopant Effect in the Photocatalytic Activity of TiO<sub>2</sub> Films Prepared by DC Reactive Magnetron Sputtering. *Vacuum*,78, 37- 46. [[Crossref](#)]
- Dantong, Z., Zhi, C., Tong, G., Feng, N., Laishun, Q., & Yuexiang, H. (2015). Hydrogen Generation from Water Splitting on TiO<sub>2</sub> Nanotube-Array-Based photocatalysts. *Energy Technology*, 3(9),888-895. [[Crossref](#)]
- Daude,N., Gout C. & Jouanin C. (1977). Electronic Band Structure of Titanium dioxide. *Physical Review B*,15, 3229. [[Crossref](#)]
- Dorian, A. H. H., Mohammed, H. N. A., Sean, L., Aibing, Y. & Charles, C. S. (2012). Ab initio Study of Phase Stability in Doped TiO<sub>2</sub>. *Computational Mechanics*. 50(2),185-194. [[Crossref](#)]
- Fujishima, A, & Honda, K. (1972). Electrochemical Photolysis of Water at a Semiconductor Electrode. *Nature*, 283: 37-38. [[Crossref](#)]
- Hao C., Xuechao L., Rundong W., Sharon K-W., & Ying L. (2017). A DFT Study of the Electronic Structures and Optical Properties of (Cr, C) Co-doped Rutile TiO<sub>2</sub>. *Chemical Physics*, 501. [[Crossref](#)]
- Howard, C. J., Sabine , T. M. & Dickson F. (1991). Structural and Thermal Parameters for Rutile and Anatase. *Acta Crystallographica*, B47, 462-468. [[Crossref](#)]
- Kominami, H., Kohno, M., & Kera, Y. (2000). Synthesis of Brookite-type Titanium Oxide Nano Crystals in Organic Media., *Journal of Materials Chemistry*, 10, 1151-1156. [[Crossref](#)]
- Landmann M., Rauls E. & Schmidt W. G. (2012). The Electronic Structure and Optical Response of Rutile, Anatase and Brookite TiO<sub>2</sub>. *Journal of Physics: Condensed Matter*, 24, 195503. [[Crossref](#)]
- Lee M.S., Hong S.S. & Mohseni M. (2005). Synthesis of Photocatalytic Nanosized TiO<sub>2</sub> -Ag Particles with Sol-gel Method Using Reduction Agent. *Journal Molecular Catalyst A*, 242, 135-140. [[Crossref](#)]
- Lettmann C., Hildebrand K., Kisch H., Macyk W. & Maier W.(2001). Visible Light Photodegradation of 4-chlorophenol with a Coke-Containing Titanium Dioxide Photocatalyst. *Applied Catalyst B*, 32, 215-227. [[Crossref](#)]
- Li X.Z, & Li F.B. (2001). Study of Au/Au<sup>3+</sup> - TiO<sub>2</sub> Photocatalysts Towards Visible Photooxidation for Water and Wastewater Treatment. *Environ 2 Science Technology*, 35, 2381-2387. [[Crossref](#)]
- Li X. Z & Li F. B. (2002). The Enhancement of Photodegradation Efficiency Using Pt-TiO<sub>2</sub> Catalyst. *Chemosphere*, 48, 1103-1111. [[Crossref](#)]
- Meesombad K., Sato N., Pitiphattharabun, S., Panomsuwan, G., Techapiesancharoenkij, R., Surawathanawises, K., Wongchoosuk, C., Boonsalee, S., Pee, J.H., Jongprateep, O. (2021). Zn-doped TiO<sub>2</sub> nanoparticles for Glutamate Sensors. *Ceramics International*, 47(15), 21099-21107. [[Crossref](#)]
- Monkhorst, H. J. & Pack, J. D. (1976). Special points for Brillouin-zone integrations. *Physical review B*, 13(12), 5188-5192. [[Crossref](#)]
- Navarra,W., Ritacco, I., Sacco, O.,Caporaso, L., Camellone,M.F., Venditto, V. & Vaiano, V. (2022). Density Functional Theory Study and Photocatalytic Activity of ZnO/N-Doped TiO<sub>2</sub> Heterojunctions. *Journal of Physical Chemistry C*, 126(16),7000-7011. [[Crossref](#)]
- Nura H., Abdu S. G., Shuaibu A. & Abubakar M. S.(2019). Electronic Band Structure and Optical Properties of Titanium dioxide. *Science World Journal*, 14(3). [scienceworldjournal.org](http://scienceworldjournal.org)
- Othmen k., Abdelkader M., & Tarek L. (2021). Theoretical and experimental investigation of the electronic, optical, electric, and elastic properties of Zn-doped anatase TiO<sub>2</sub> for photocatalytic applications. *Applied Physics A*, 127-557. [[Crossref](#)]

- Paola, G., Stefano, B., Nicola, B., Matteo, C., Roberto, C., Carlo, C., Davide, C., Guido, L. C., Matteo, C., & Ismail, D. (2009). Quantum ESPRESSO: A Modular and Open-Source Software Project for Quantum Simulation of Materials. *Journal of Physics: Condensed Matter*, 21, 395502. [\[Crossref\]](#)
- Pascual, J., Camassel, J. & Mathieu H. (1978). Piezospectroscopic Investigation of Nature of the Subsidiary Valence Band Extrema in TiO<sub>2</sub>. *Solid State Communications*. 28(3), 239-241. [\[Crossref\]](#)
- Qing, G., Chuanyao, Z., Zhibo, & M., Xueming, Y. (2019). Fundamentals of TiO<sub>2</sub> Photocatalysis: Concepts, mechanisms and challenges. *Advanced Materials*, 3(50), 1901997. [\[Crossref\]](#)
- Rauf, M.A., Meemani, M. A. & Hisaindee, S. (2011). An Overview on the Photocatalytic Degradation of Azo Dyes in the Presence of TiO<sub>2</sub> Doped with Selective Transition Metals. *Desalination*, 276, 13-27. [\[Crossref\]](#)
- Sasanka, P., Haritha, B. D., Kumudu, N. R., Sanjaya, V. B. & Ishanie, R. P. (2021). Recent Development and Future Prospects of TiO<sub>2</sub> Photocatalysis. *Journal of the Chinese Chemical Society*, 68(5), 738-769. [\[Crossref\]](#)
- Sharma, S. B., Qattan, I. A., Jaoude, M.A. & Abedrabbo, S. (2023). First-Principles DFT Study of Structural, Electronic and Optical Properties of Cu-doped TiO<sub>2</sub> (112) Surface for Enhanced Visible-Light Photocatalysis. *Computational Materials Science*, 218, 111952. [\[Crossref\]](#)
- Tang, H., Prasad, K., Sanjines, R., & Levy, F., (1995). TiO<sub>2</sub> Anatase Thin Films as Gas Sensors. *Sensors and Actuators B: Chemical*, 26, 71-75. [\[Crossref\]](#)
- Takeshita K, Yamakata A, Ishibashi T, Onishu H, Nishijima K, Ohno T. & Transient I.R. (2006). Absorption Study of Charge Carriers Photo-Generated in Sulfur-Doped TiO<sub>2</sub>. *Journal of Photochem Photobiol*, 177, 269-275. [\[Crossref\]](#)
- Takeshi M., Ryoji A., Takeshi O., Koyu A. & Yasunori T. (2001). Band-gap Narrowing of Titanium Dioxide by Nitrogen Doping. *Japanese Journal of Applied Physics*, 40, L561. [\[Crossref\]](#)
- Treschev S.Y, Chou P.W, Tseng T.H, Wang J.B, Perevedentseva E.V, Cheng C.L. (2008). Photoactivities of the Visible Light-Activated Mixed-Phase Carbon-Containing Titanium Dioxide: The Effect of Carbon Incorporation. *Applied Catalyst B*, 79, 8-16. [\[Crossref\]](#)
- Tunkay D., Ozan, Y., Alper, A., Selim, D., Serdar, G., Serdar & Y., Metin Y. (2022). Production of Zn-doped TiO<sub>2</sub> Film with Enhanced Photocatalytic Activity. *Journal of the Australian Ceramic Society*, 58, 1415-1421. [\[Crossref\]](#)
- Vivek C., Pau F. & Mingming T. (2023). First-principles study of electronic properties of Zn and La doped and co-doped anatase TiO<sub>2</sub>. *AIP Advances* 13, 125013. [\[Crossref\]](#)
- Wu Z, Dong F, Zhao W, & Guo S. (2008). Visible Light Induced Electron Transfer Process Over Nitrogen Doped TiO<sub>2</sub> Nanocrystals Prepared by Oxidation of Titanium Nitride. *J Haz Mat.*, 157(1), 57-63. [\[Crossref\]](#)
- Wu J.C-S, & Chen C.H. (2004). A Visible-Light Response Vanadium-Doped Titania Nanocatalyst by Sol-gel Method. *J Photochem Photobiol A*, 163: 509-515. [\[Crossref\]](#)
- Yu J, Zhou M, Cheng B, & Zhao X. (2006). Preparation, Characterization and Photocatalytic Activity of In situ N, S-codoped TiO<sub>2</sub> Powders. *J Mol Catal A*, 246, 176-184. [\[Crossref\]](#)
- Zaleska A, Sobczak JW, Grabowska E. & Hupka J. (2007). Preparation and Photocatalytic Activity of Boron-Modified TiO<sub>2</sub> Under UV and Visible Light. *Appl Catal B*, 78, 92-100. [\[Crossref\]](#)
- Zhang, C., Wang, C-L., Li, J.-C. & Yang, K. (2007). Structural and electronic properties of Fe-doped BaTiO<sub>3</sub> and SrTiO<sub>3</sub>. *Chinese physics*, 16(5), 1422-1428. [\[Crossref\]](#)